Article

Removal of Azo Dyes from Water Using Natural *Luffa cylindrica* as a Non-Conventional Adsorbent

Ma. Guadalupe Aranda-Figueroa [1], Adriana Rodríguez-Torres [2], Alexis Rodríguez [3], Gloria Ivette Bolio-López [4], David Osvaldo Salinas-Sánchez [5], Dulce Ma. Arias-Atayde [6], Rosenberg J. Romero [7,*] and Maria Guadalupe Valladares-Cisneros [1,*]

1   Facultad de Ciencias Químicas e Ingeniería, Universidad Autónoma del Estado de Morelos, Avenida Universidad 1001, Colonia Chamilpa, Cuernavaca 62209, Mexico; ma.arandafgr@uaem.edu.mx
2   Departamento de Ingeniería en Aeronáutica, Universidad Politécnica Metropolitana de Hidalgo, Tolcayuca 1009 Ex Hacienda San Javier, Tolcayuca 43860, Mexico; adrodriguez@upmh.edu.mx
3   Centro de Investigación en Biotecnología, Universidad Autónoma del Estado de Morelos, Avenida Universidad 1001, Colonia Chamilpa, Cuernavaca 62209, Mexico; alexis.rodriguez@uaem.mx
4   Dirección de Ciencias Básicas e Ingeniería, Universidad Popular de la Chontalpa, Carretera Cardenas-Huimanguillo Km 2.0, Cardenas 86500, Mexico; gloria.bolio@upch.mx
5   Centro de Investigación en Biodiversidad y Conservación, Universidad Autónoma del Estado de Morelos, Avenida Universidad 1001, Colonia Chamilpa, Cuernavaca 62209, Mexico; davidos@uaem.mx
6   Centro de Investigación y Educación Ambiental Sierra de Huautla (CEAMISH), Universidad Autónoma del Estado de Morelos, Avenida Universidad 1001, Colonia Chamilpa, Cuernavaca 62209, Mexico; dulce@uaem.mx
7   Centro de Investigación en Ingeniería y Ciencias Aplicadas, Universidad Autónoma del Estado de Morelos, Avenida Universidad 1001, Colonia Chamilpa, Cuernavaca 62209, Mexico
*   Correspondence: rosenberg@uaem.mx (R.J.R.); mg.valladares@uaem.mx (M.G.V.-C.)

Abstract: Reducing high concentrations of pollutants such as heavy metals, pesticides, drugs, and dyes from water is an emerging necessity. We evaluated the use of *Luffa cylindrica* (*Lc*) as a natural non-conventional adsorbent to remove azo dye mixture (ADM) from water. The capacity of *Lc* at three different doses (2.5, 5.0, and 10.0 g/L) was evaluated using three concentrations of azo dyes (0.125, 0.250, and 0.500 g/L). The removal percent (R%), maximum adsorption capacity (Q_m), isotherm and kinetics adsorption models, and pH influence were evaluated, and Fourier-transform infrared spectroscopy and scanning electron microscopy were performed. The maximum R% was 70.8% for 10.0 g L^{-1} *Lc* and 0.125 g L^{-1} ADM. The Q_m of *Lc* was 161.29 mg g^{-1}. Adsorption by *Lc* obeys a Langmuir isotherm and occurs through the pseudo-second-order kinetic model. Statistical analysis showed that the adsorbent dose, the azo dye concentration, and contact time significantly influenced R% and the adsorption capacity. These findings indicate that *Lc* could be used as a natural non-conventional adsorbent to reduce ADM in water, and it has a potential application in the pretreatment of wastewaters.

Keywords: *Luffa cylindrica*; unmodified fiber; non-conventional adsorbent; azo dyes; dye removal

1. Introduction

Processing and manufacturing industries are sources of generated wastewater, which includes a mixture of pollutants, including heavy metals, pesticides, azo dyes, drugs, and oils. Wastewater can be classified depending on the type of compounds it contains. For instance, according to the World Bank, textile dyeing generates between 17% and 20% of industrial wastewater [1]. Mainly, textile wastewater contains dyes and salts and largely aqueous soluble inorganic-colored complexes. Some authors have reported that wastewater from the leather industry may contain up to 200 mg L^{-1} of dyes [2].

Most color-based industries commonly employ, at the end of the process, a wastewater treatment to reduce the pollutant concentrations before leaving water in open sources.

However, the complexity and heterogeneity of the pollutants in wastewater need highly efficient technologies. Hence, water treatment plants are closely monitored and regulated by standard protocols to meet the required standards for water quality [3]. Higher pollutant concentration disposed in water is correlated with a huge risk and hazardous impacts on the environment and human health [2,4]. Consequently, water treatment is a leading factor in the accomplishment of sustainable water provision [5].

The presence of dyes in water is highly visible. Moreover, even at concentrations of <1.0 mg L^{-1} [6], there can be significant changes in the physicochemical properties of water. For example, dyes reduce the transmission and penetration of sunlight into the water and thus affect the biochemical oxygen demand (BOD), chemical oxygen demand (COD), and pH [7,8]. Synthetic textile dyes are widely used due to their easy application and ability to give clothing brighter and more durable colors [9].

Azo dyes are the largest and the most important group of synthetic dyes [10]. They are highly toxic and stable under different environmental conditions (light, heat, etc.) and resist degradation processes (aerobic digestion and oxidizing agents) [11].

Several technologies are being studied as part of wastewater treatment, including the combination of pre-treatments and primary treatments to reduce the organic load and improve the efficiency of secondary processes [12]. The most acceptable approaches should be eco-friendly and non-polluting. Moreover, the removal techniques that are used should consider the types of pollutants and their concentration [13].

Adsorption is a widely accepted technique because it is easy to apply, efficient for pollutant removal, does not require supplements, and can be low cost when a natural absorbent is applied [13–15]. The adsorbent, a highly porous material, has a large surface area and many free functional groups that provide adequate and selective adsorption [16–18]. To ensure sustainability in wastewater treatment, for nearly two decades, natural sources have been studied as non-conventional adsorbent materials to remove or reduce pollutants in water, including dyes; they have demonstrated good adsorption capacity [19,20]. For example, Acid Blue 25 was removed using waste tea residue (50.8 mg g^{-1}) [21]. Crystal violet and methylene blue were removed using sugarcane bagasse (107.5 and 112.9 mg g^{-1}, respectively) [22]. Malachite green was removed by employing grape stalks (214.1 mg g^{-1}) [23]. Methyl red was removed using eggshell powder (1.26 mg g^{-1}) [24]. Cibacron blue was removed by utilizing pistachio shells (1.63 mg g^{-1} untreated and 4.53 mg g^{-1} chemically treated) [25]. Crystal violet was removed using activated carbon from pomegranate peels (23.26 mg g^{-1}) [26]. Tartrazine was removed with activated carbon powder from cola nut shells (19.26 mg g^{-1}) [27]. While these reports show that non-conventional adsorbents represent emerging and eco-friendly alternatives for water decontamination, most of them focused on the removal of only one dye. The purpose of the present study was to establish the adsorption capacity of the non-conventional natural and green material *Luffa cylindrica* (*Lc*) to remove an azo dye mixture.

2. Results

2.1. Azo Dye Mixture Removal

Figure 1 shows the removal of ADM, considering 2.5, 5.0, and 10.0 g L^{-1} *Lc* doses.

2.2. The Effect of pH

The effect of pH is shown in Figure 2. pH 2.0 led to the lowest ADM removal (47.3%); there was 60–70% ADM removal at pH 4.0–8.0. The highest removal (79.3%) occurred at pH 3.0.
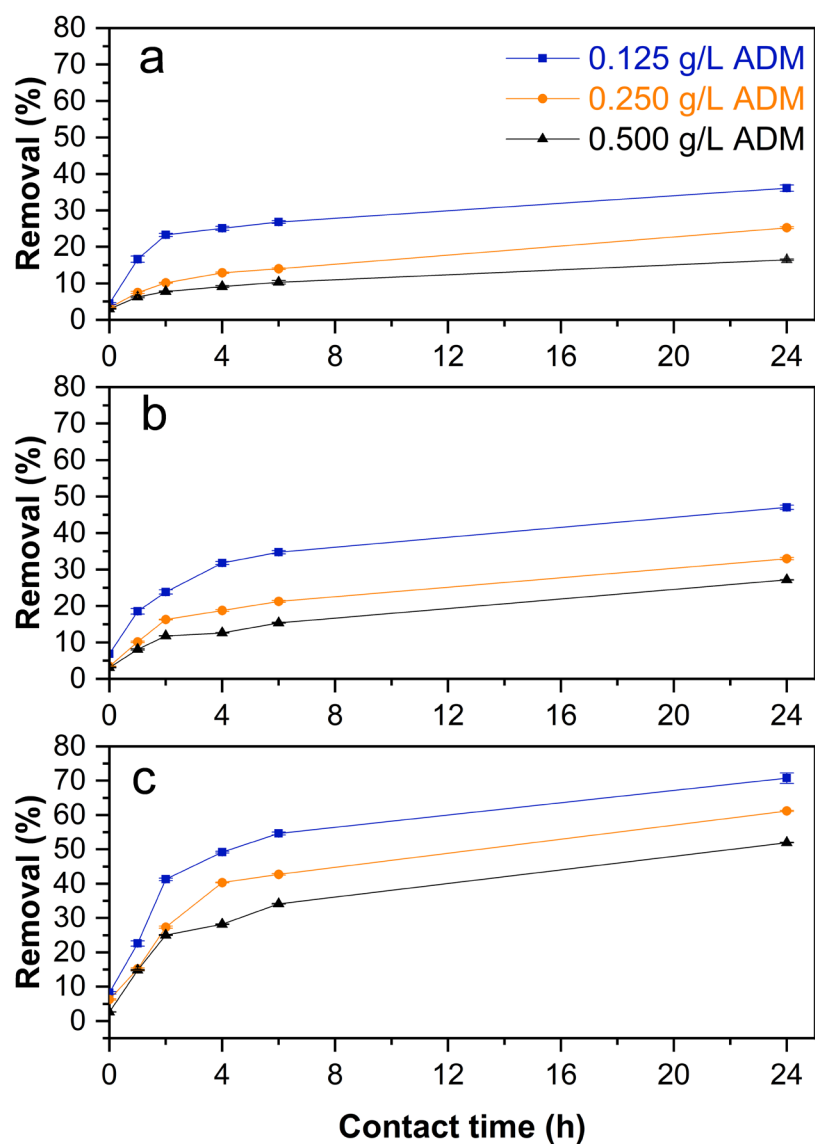
Figure 1. Removal of ADM using (**a**) 2.5; (**b**) 5.0; (**c**) 10 g L^{-1} of *Lc*.
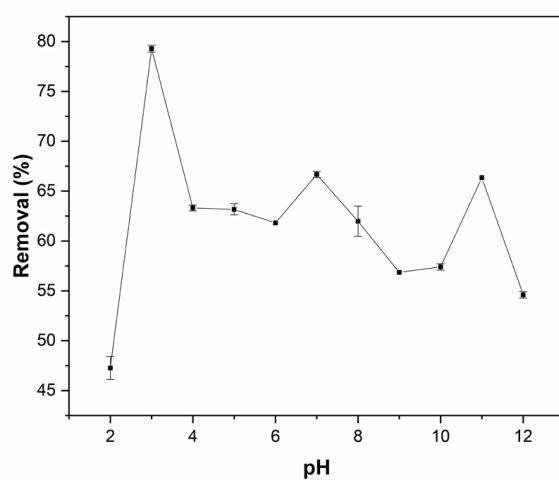
Figure 2. Effect of pH in ADM removal using *Lc* (adsorbent dose: 2.5 g/L, C$_0$: 0.250 g L^{-1}).

2.3. Adsorption Capacity

The adsorption capacity for 2.5, 5.0 and 10.0 g L^{-1} *Lc* dose is showing in Figure 3a. The time effect respect to adsotprion capacity for 2.5 g L^{-1} *Lc* is showing in Figure 3b.
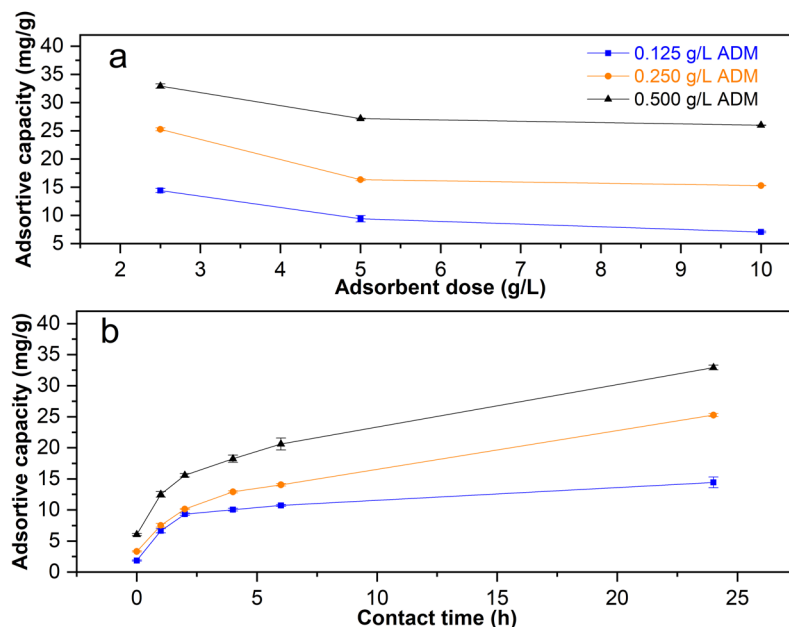

Figure 3. (**a**) Effect of the adsorbent dose and (**b**) effect of contact time on *Lc* adsorptive capacity (Q).

The relation between concentration (C_e) at the equilibrim and adsorption capacity (Q_e), starting from 0.5 g L^{-1} ADM, are showing in Figure 4.
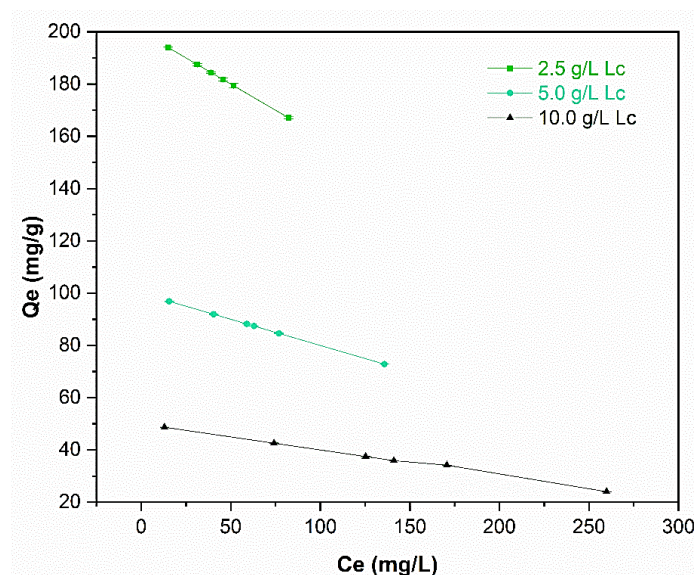

Figure 4. Concentration (C_e) versus adsorptive capacity at the equilibrium (Q_e).

2.4. Adsorption Isotherms

Figure 5 shows how the adsorption isotherms fit the data. According to the correlation coefficient (R^2) values, the Langmuir model (Figure 5a) provided the best fit. Thus, ADM adsorbs to the *Lc* surface by forming a homogeneous monolayer.
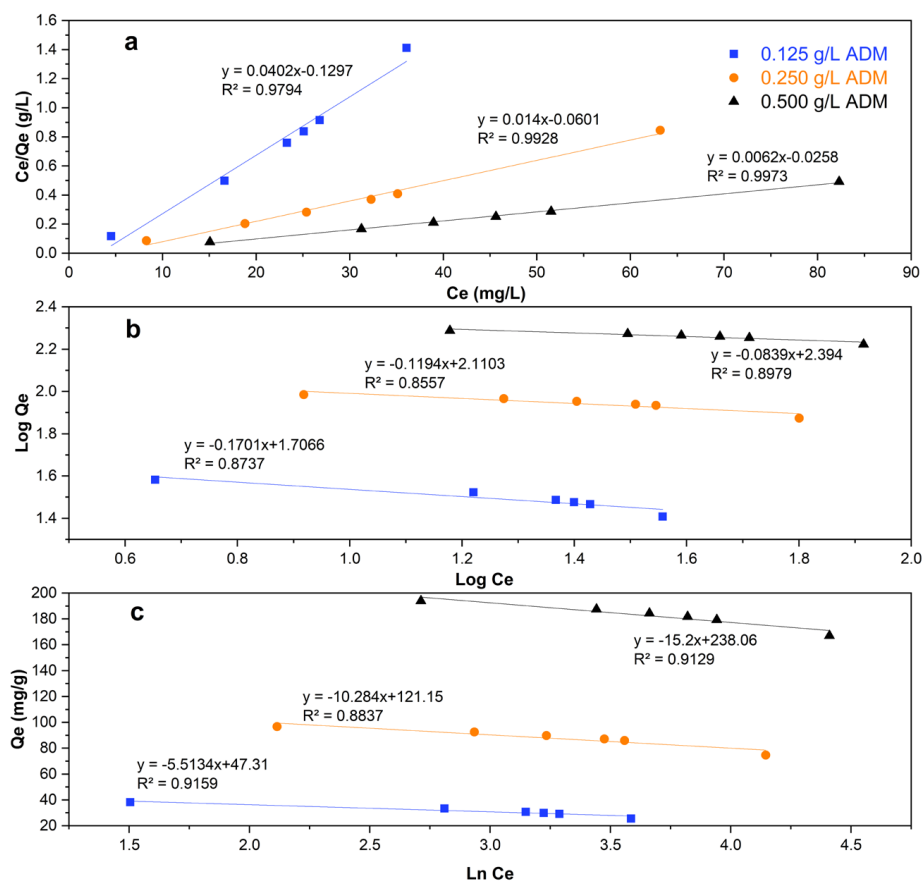
Figure 5. Langmuir (**a**), Freundlich (**b**), and Temkin (**c**) isotherm models for the adsorption of ADM (*Lc* dose: 2.5 g L^{-1}).

2.5. Adsorption Kinetics

The kinetic parameters from the models evaluated using 2.5 g L^{-1} *Lc* are presented in Table 1, and Figure 6 shows the best fit for the data. Table 2 compares the results from the present study with other adsorption studies using *Luffa* spp. to remove dyes in water [28–33].

Table 1. Kinetic parameters of the adsorption of ADM using *Lc* (ADM = 0.125 g L^{-1}, *Lc* = 2.5 g L^{-1}, t = 24 h, T = 298 ± 2 °K; pH = 7.0).

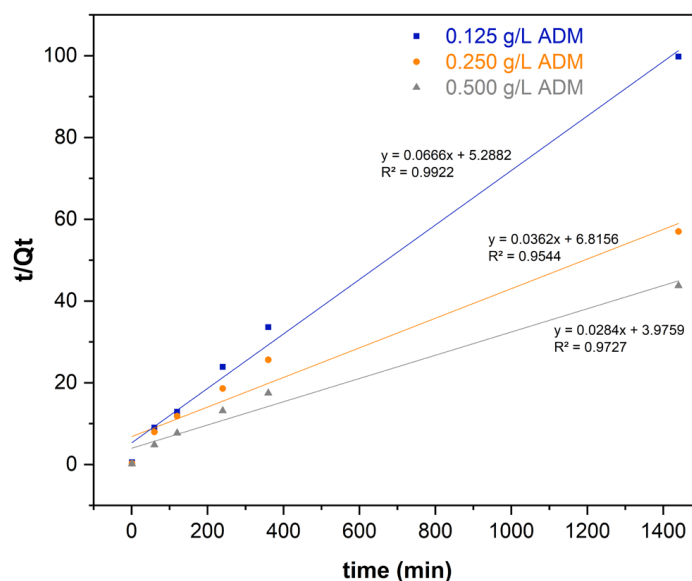| Kinetic Model	Parameters	Value	R^2
Pseudo-first order	k_1 (min^{-1})	−0.0007	0.7974
	Q_e, observed	24.8756	
	Q_e, calculated	26.7384	
Pseudo-second order	k_2 (g min mg^{-1})	0.0008	0.9922
	Q_e, calculated	15.0150	
Intraparticle diffusion	k_{id} (mg min$^{1/2}$ g^{-1})	0.3085	0.8456
	C	4.0895	
Elovich	B (g mg^{-1})	0.5967	0.9595

Figure 6. Pseudo-second order model for the kinetic adsorption of ADM (*Lc* dose: 2.5 g L^{-1}).

Table 2. Adsorption studies with *Luffa* spp. as adsorbent for dye removal.

Study	Adsorbent (g L^{-1})	Dye (mg L^{-1})	pH	T (°K)	t (h)	Q$_m$ (mg g^{-1})	Isotherm Model	k$_2$ (g mg^{-1}min^{-1})	R^2	Reference
MG-*Lc*	0.05	20	5.0	308	5.0	29.40	L	0.013	0.996	[33]
MG-*Lap*	0.6	50	7.0	303	2.5	166.67	L	0.003	0.995	[31]
TB-*Lc*	1	10	7.0	303	0.5	45.60	L	0.0029	0.919	[29]
AB-*Lc*	1	20	2.0	293	4.0	9.63	F and T	0.004	0.999	[28]
MB-*Lc*	3	300	5.8	293	25.0	49.46	L	0.0051	0.999	[30]
MG-*Lap*	8	50	4.0	323	3.0	69.64	L	3.615	0.999	[32]
This study	2.5	125	7.0	298 ± 2	24	24.88	L	0.0008	0.992	This study
		250				71.43		0.0002	0.954	
		500				161.29		0.0002	0.973	

Lc: *Luffa cylindrical*; *Lap*: *Luffa aegyptica* peel; TB: Trypan Blue; AB: Alpacide Blue; MG: Malachite Green; MB: methylene blue; L: Langmuir; F: Freundlich; T: Temkin.

2.6. FTIR Spectroscopy

FTIR spectra (Figure 7) were acquired to analyze *Lc* with and without ADM and ADM only.

2.7. Morphology of Lc

The analysis of FESEM micrographs of the *Lc* surface before and after ADM adsorption is shown in Figure 8.

Based on energy-dispersive X-ray spectroscopy analysis (EDXA), before adsorption, *Lc* (Figure 8c) was composed of 56.2% carbon and 38.2% oxygen (Table 3).
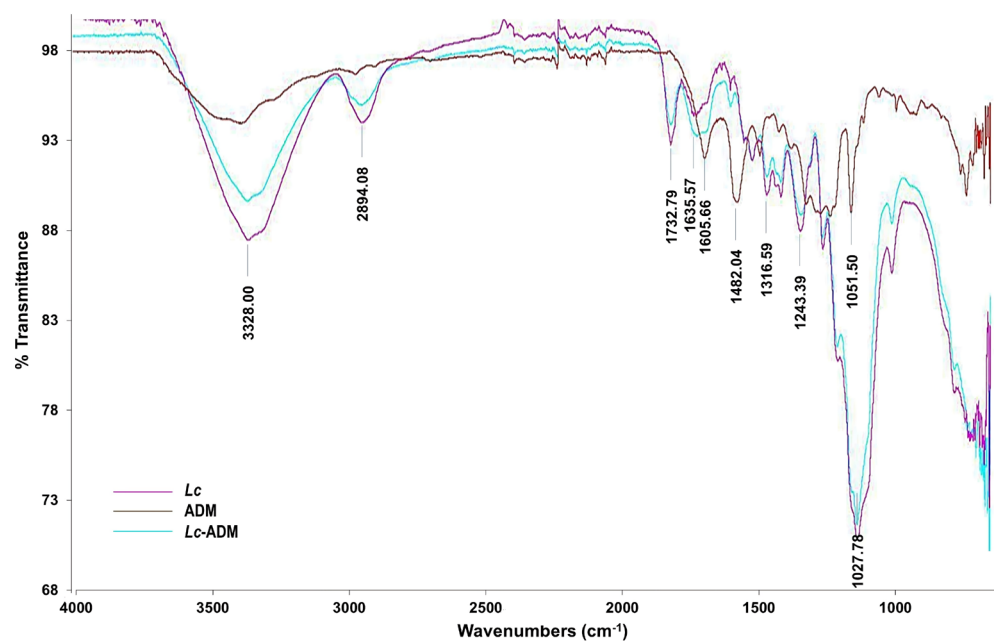
Figure 7. FTIR spectra of non-conventional and untreated *Lc* (pink line), ADM (reddish-brown line), and ADM adsorbed to *Lc* (blue-green line).
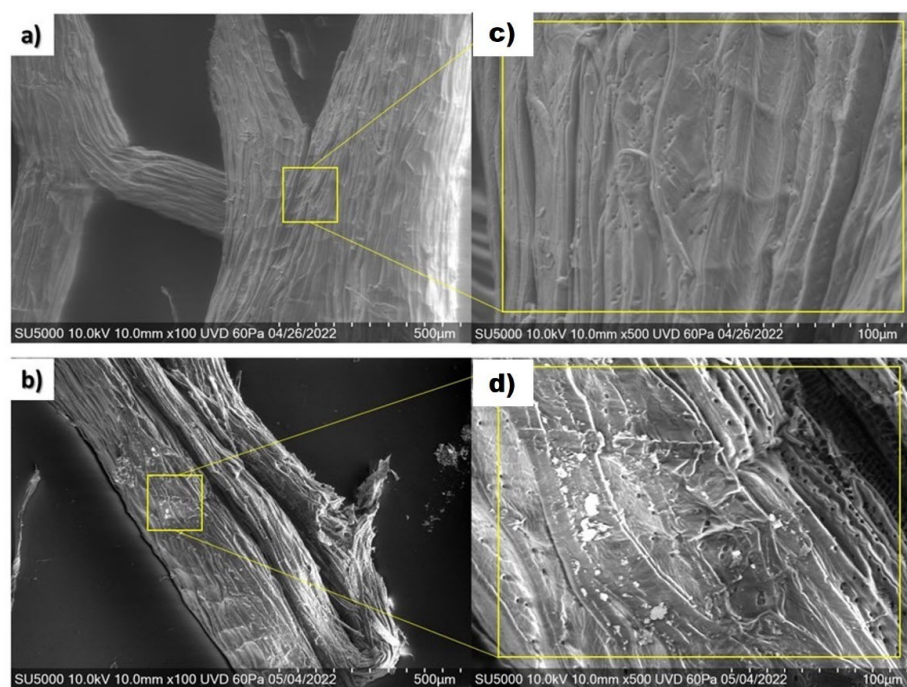

Figure 8. FESEM micrographs of (**a**) untreated natural *Lc*, (**b**) *Lc* after ADM adsorption, (**c**) amplification of untreated *Lc* (500), (**d**) amplification of *Lc* after ADM adsorption (500).

Table 3. Principal elements identified on the biomass surface by FESEM/EDXA.

Material	Element Content (%)					
	C	**N**	**O**	**Na**	**Al**	**Si**
Untreated *Lc*	56.2	N.D.	38.2	N.D.	5.2	0.4
Lc-ADM	53.4	15.2	24.7	0.8	4.6	0.4

N.D. No detected

3. Discussion

After 24 h as contact time, the highest *Lc* dose (10.0 g L^{-1}) had removed 70.8% of ADM azo dye (line blue, Figure 1c). Based on previous studies, other lignocellulosic adsorbents could remove approximately 90% of dyes; however, most of these studies focused on only one dye or used chemically modified adsorbents [34–36].

pH is a crucial parameter in the adsorption process [37,38] because it impacts the binding sites on the adsorbent and alters the electronic environment of dissolved molecules. In acidic media, the surface is positively charged, and H$^+$ ions compete with dye cations, meaning that less adsorbent interacts with the adsorbate [39,40]. On the other hand, in basic media, the lignin and cellulose chains of *Lc* fibers become negatively charged, and thus, the azo dyes cannot interact well with the adsorbent. Analysis of variance showed that pH significantly affects ADM removal ($p < 0.05$).

The adsorption capacity is enhanced at the lowest *Lc* dose and the highest ADM concentration (Figure 3a), and it increases with respect to time (Figure 3b). The highest Q$_e$ was obtained when using 2.5 g L^{-1} *Lc*.

The adsorption of ADM along the entire surface of *Lc* is mediated by the formation of multiple, different, and strong physicochemical interactions like van der Waals forces [41]. Similar observations have been reported when using natural adsorbents from agricultural waste such as *Citrus limetta* peel [42], wheat straw [43], shaddock husk [44], and cotton-seed husk [45], to mention a few examples, to remove dyes in solution. In each of the aforementioned studies, the Langmuir isotherm provided the best fit for the data.

According to the R^2 values (Table 1 and Figure 6), the pseudo-second-order model shows the best fit for the data. Hence, the removal process involves chemisorption [28]. In most of them, the Langmuir isotherm and the pseudo-second-order model best described the dye adsorption processes, even with other pollutants or adsorbents [14,46–48].

Unmodified *Lc* (green line, Figure 7) shows a broad absorption band at 3328 cm^{-1} characteristic of O–H. A broad shorter peak at 2894 cm^{-1} is attributable to C–H stretching vibrations. The bands at 1370, 1317, and 1243 cm^{-1} represent vibrations for –CH– and –CH$_2$– groups [49]. The peaks at 1620 and 1424 cm^{-1} show conjugated double bonds. The strong peak at 1027 cm^{-1} is attributed to C–O–C and to C–O vibrations, bonds present in polysaccharides [50]. All these signals describe a lignocellulosic material [51]. The FTIR spectrum of ADM (blue line, Figure 7) shows the vibrations of the π conjugation system of C=C bending (1606 cm^{-1}) and of N=N stretching (1482 cm^{-1}), characteristics of amines. The sulfonate group vibrations are observed at 1396 cm^{-1} (the S=O double bond) and 1052 cm^{-1} (the S–O bond) [52]. A broad signal at 3354 cm^{-1} is attributed to N–H bonds for amines. The FTIR spectra of ADM adsorbed to *Lc* (reddish-brown line, Figure 7) show a broad signal at 3332 cm^{-1} assigned to N–H and O–H vibrations due to dye–adsorbent interactions. The azo group (–N=N) vibrates at 1580 cm^{-1}, as confirmed by stretching vibrations at 1243 and 1158 cm^{-1}. The signals at 1405, 1316, and 1031 cm^{-1} indicate the stretching vibrations for the sulfonate group present in the dye [53].

FTIR signals corresponding to hydroxyl, carbonyl, and alkyl functional groups, and aromatic vibrations are generally present in cellulose, hemicellulose, and lignin [54,55]. All of those vibrations are present in the *Lc*–ADM FTIR spectrum (reddish-brown line, Figure 7). Moreover, the peaks at 3328, 2894, and 1732–1482 cm^{-1} indicate that ADM involves stronger interactions with the hydroxyl and carbonyl groups of *Lc* and methylene hydrogens of the aromatic ring of ADM dye on the *Lc* surface.

Figure 8c (enclosed zone in yellow) shows the fibrous structure of *Lc* with many small holes (0.5–4 μm in diameter). The smooth amorphous waxy/gummy layer indicates the presence of lignin [56]. Porosity increases the surface area of adsorbent material [17]. Figure 8d (enclosed zone in yellow) shows the changes in the surface of *Lc* after ADM adsorption. It is possible to observe that the holes are occupied by the ADM molecules. The large, brilliant zones could correspond to salts [42,57].

The data of composition *Lc* obtained by EDXA (Table 3) are consistent with the composition of cellulosic and hemi-cellulosic materials [15]. After adsorption (Figure 8d),

Lc exhibited a composition of 53.4% carbon, 15.2% nitrogen, and 24.7% oxygen as the chief elements, along with trace amounts of other elements.

Thus, azo dye mixture likely adsorbs to *Lc* via hydrogen, electrostatic, chemical, and van der Waals interactions [54,58]. In the literature, researchers have reported various adsorption mechanisms depending on the chemical composition of the adsorbent, the nature of the pollutant, and the environmental media [11,18,59]. The adsorption process in solution involves water molecules forming hydrogen bonds between dyes and free functional groups on the *Lc* lignin–cellulose surface [60–62]. In agreement with the results of the isotherms and the FTIR spectra of the adsorbent after ADM adsorption, it is necessary to consider that the molecules and free ions play an important role in the adsorption process. Figure 9 shows a general mechanism for the *Lc*–ADM interaction to understand how adsorption occurs.
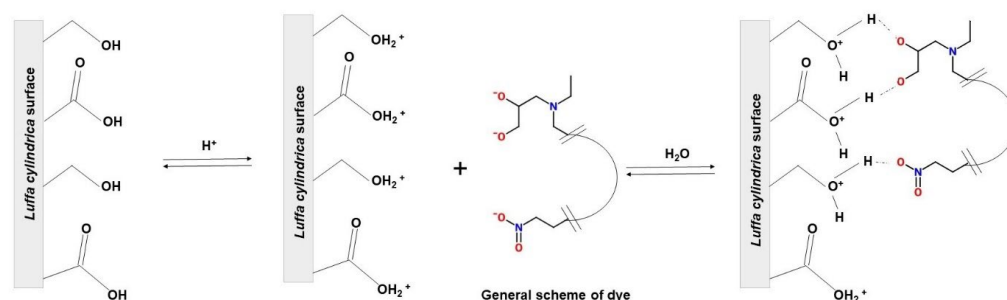

Figure 9. Mechanism of adsorption proposal to *Lc*-ADM in aqueous solution.

4. Materials and Methods

4.1. Luffa Cylindrica (Lc)

Lc (Figure 10) is a fibrous, highly porous natural material composed of lignocellulose [13]. It has a large surface area with a large number of hydroxyl groups that can bind organic and inorganic molecules [63,64]. Dried *Lc* was acquired from Buenavista de Cuellar, Guerrero, Mexico (18°27′32″ N 99°24′20″ W). It was cleaned, the peel and seeds were removed, and it was cut into small 1 cm^3 fragments, which were exhaustively washed using distilled water and dried using an oven (RIOSSA made in Mexico) at 40 °C for 24 h. These *Lc* fragments were used in the subsequent experiments as untreated natural fiber.

Figure 10. *Luffa cylindrica*; longitudinal and cross-sectional views of its structure.

4.2. Azo Dye Mixture

A commercial mixture of azo dyes commonly used to renew the blue color of jeans at home was acquired from a local supermarket; the commercial mixture is commonly named 'Indigo Blue'. Its formulation contains nine azo dyes: blue 71, 86, 102, 151, 200, and 201; black 22; red 23; and yellow 50 (Figure 11) as the major ingredients. They can be classified as mono-, di-, tri-, and tetra-azo dyes, one of which is a phthalocyanine class. This commercial azo dye mixture was renamed as 'Azo dye mixture' (ADM). A stock solution

of ADM (1.0 g L^{-1}) was prepared and used for all experiments. The maximum absorbance of ADM was determined using an ultraviolet–visible (UV–vis) spectrophotometer; it was detected at 550 nm.
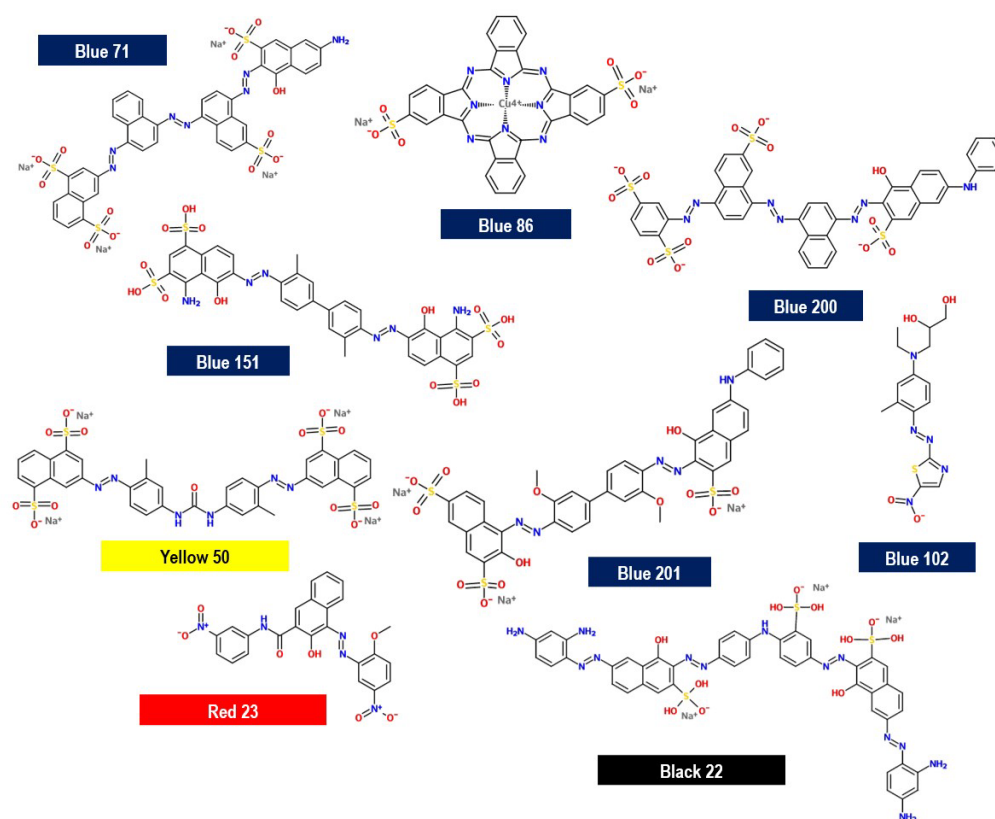

Figure 11. Chemical structure of dyes contained in ADM. Description: Monoazo dye: Disperse Blue 102 and Direct Red 23; Diazo dye: Direct Blue 151 and 201 and Direct Yellow 50; Triazo dye: Direct Blue 71 and Disperse Blue 200; Tetra-azo dye: Direct Black 22; and Phthalocyanine dye: Direct Blue 86.

4.3. Experimental Design

In prior studies of adsorbents, researchers have generally used azo dye concentrations <0.100 g L^{-1} [28–30,65]. However, in real-world scenarios, dye concentrations are commonly >0.100 g L^{-1}. For this study, it was necessary to establish a factorial experimental design for batch adsorption kinetic assays considering several azo dye and *Lc* doses (Table 4).

Table 4. Experimental design.

Independent Variables	Level of Significance		
	Low (−1)	Medium (0)	High (+1)
Lc (g L^{-1})	2.5	5.0	10.0
ADM (g L^{-1})	0.125	0.250	0.500

4.4. Adsorption Kinetics

The experiments were carried out in conical borosilicate glass flasks with a 50 mL working volume in static conditions at 28 ± 2 °C and pH 7.0; the contact time was 24 h. The residual ADM concentration was measured at 550 nm. All experiments were performed in quadruplicates, and the results were processed using Origin Pro-8 version 2018 and Minitab version 20 software.

The removal percent (R%) of ADM was calculated with Equation (1):

$$R\% = \frac{C_0 - C_f}{C_0} \times 100 \tag{1}$$

where C_0 is initial concentration, C_f is final concentration, and R% is the removal percent.

The adsorption kinetics was evaluated to understand ADM removal. The amount of ADM adsorbed by *Lc* (mg g^{-1}) was calculated with Equation (2):

$$Q = \frac{C_0 - C_f}{m} \times V \tag{2}$$

where Q is the adsorption capacity (mg g^{-1}), C_0 and C_f are the initial and final concentrations (mg L^{-1}), respectively, V is the volume (L) used, and m is the *Lc* mass (g) employed [28].

Several kinetic models were analyzed with the degree of adsorption controlled as a function of time. Equation (3) was used for the pseudo-first-order model:

$$\ln(Q_e - Q_t) = \ln Q_e - k_1 t \tag{3}$$

where Q_t is the ADM amount adsorbed by *Lc* at time t (mg g^{-1}), and k_1 is the adsorption rate constant (min^{-1}).

The pseudo-second-order kinetic assumes that chemisorption is the rate-limiting step; it is represented in Equation (4) [34,42]:

$$\frac{t}{Q_t} = \frac{1}{k_2 Q_e{}^2} + \frac{t}{Q_e} \tag{4}$$

where t is the time (min), and k_2 is the rate constant of pseudo-second order (g min mg^{-1}).

Weber and Morris [66] proposed a theory based on interparticle diffusion and mentioned that adsorption occurs through a diffusion mechanism, as represented by Equation (5):

$$Q_t = k_{id} t^{1/2} + C \tag{5}$$

where k_{id} is a rate constant of intraparticle diffusion (mg min$^{1/2}$ g^{-1}), and C is a dimensionless constant.

The Elovich model provides an explanation for adsorption of an adsorbate on the surface of an adsorbent. This model assumes that adsorbents have heterogeneous active sites with different active energies [67]. The model is represented in Equation (6):

$$Q_t = \frac{\ln(\alpha\beta)}{\beta} + \frac{1}{\beta} \ln t \tag{6}$$

where α (mg g^{-1} min^{-1}) is initial adsorption rate, β (g mg^{-1}) is desorption constant, and t (min) is time [67,68].

4.5. Adsorption Isotherms

Adsorption equilibrium was analyzed to determine the adsorption capacity of *Lc* for ADM in aqueous solution. The amount of ADM adsorbed at equilibrium is expressed by Equation (7):

$$Q_e = \frac{C_0 - C_e}{m} \times V \tag{7}$$

where Q_e and C_e are the adsorption capacity and adsorbate concentration at equilibrium, respectively.

The type of adsorbent–adsorbate interaction, as well as the experimental conditions, is vital to determine which isotherm best fits the data. The equilibrium data were analyzed by considering the linearized Langmuir, Freundlich, and Temkin isotherms. The Langmuir

isotherm has been commonly used to discuss various adsorbate–adsorbent combinations (liquid and gas phase adsorption) [29,30,65,69] and is represented by Equation (8):

$$\frac{C_e}{Q_e} = \frac{1}{Q_m K_L} + \frac{1}{Q_m} C_e \tag{8}$$

where Q_e (mg g^{-1}) is the adsorption capacity of the material at equilibrium; Q_m (mg g^{-1}) is the maximum adsorption capacity to form a complete monolayer on the surface at the adsorbate concentration at equilibrium C_e (mg L^{-1}); and K_L (L mg^{-1}) is the Langmuir constant related to the affinity between the adsorbate and adsorbent [26].

The essential characteristics of the Langmuir isotherm model are known as the separation factor RL, which can be expressed by Equation (9):

$$R_L = \frac{1}{1 + K_L C_0} \tag{9}$$

If R_L is > 1, the adsorption is unfavorable. The adsorption is linear if R_L is 1. When R_L is >0 but <1, the absorption is favorable. Finally, if R_L is 0, then absorption is irreversible [31].

The Freundlich isotherm is represented by Equation (10):

$$\log Q_e = \frac{1}{n} \log C_e + \log K_F \tag{10}$$

where K_F is the Freundlich constant [(mg g^{-1}) (L mg^{-1})$^{1/n}$], and n is a dimensionless constant that is related to the absorption intensity of the adsorbent–adsorbate relationship, sometimes called the adsorption intensity or surface heterogeneity [26,70].

The Temkin isotherm is presented in Equation (11):

$$Q_e = B * Ln C_e + B * Ln K_T \tag{11}$$

where B (J mol^{-1}) is the Temkin constant, obtained from RT/b, where R is the universal gas constant (8.314 J mol^{-1}), T is the temperature in Kelvin (298 $^\circ$K), b is the variation in the absorption energy, and K_T is the Temkin equilibrium constant (L mg^{-1}) [70].

4.6. Influence of pH on ADM Removal

The pH effect of ADM removal was evaluated. A solution of 0.500 g L^{-1} ADM was prepared using 0.01 M KNO$_3$ as a buffer [28,30]. Then, the pH was adjusted between 2 and 12 by adding 0.1 M NaOH or HCl. *Lc* (2.5 g L^{-1}) was added to each flask and incubated for 24 h. Samples were taken at 0 and 24 h and analyzed to calculate the percent ADM removal.

4.7. Fourier-Transform Infrared (FTIR) Spectroscopy

FTIR spectra were obtained with a Spectrum One FTIR spectrophotometer (Perkin Elmer, Wellesley, MA, USA). The spectra included 128 scans from 500 to 4000 cm^{-1} at a resolution of 4 cm^{-1}.

4.8. Field Emission Scanning Electron Microscopy (FESEM)

The internal three-dimensional (3D) morphology and the surface of *Lc* before and after dye adsorption were obtained with FESEM coupled to energy-dispersive X-ray spectroscopy using a Hitachi SU5000 microscope manufactured in Tokio, Japan. The fiber samples were sprayed with gold coating, and the analysis of samples was acquired by topographic contrast and registered at 100 and 500 magnification.

5. Conclusions

Lc could remove 70.8% of ADM dissolved in water in static conditions at 25 $\pm$ 2 $^\circ$C, pH 7.0, and a contact time of 24 h. The adsorption capacity of *Lc* was 161.29 mg g^{-1};

adsorption occurs according to the Langmuir isotherm, and the kinetics obeys the pseudo-second-order model. The statistical analysis showed that the adsorbent dose, the azo dye mixture concentration, pH, and contact time significantly influence azo dye mixture removal and the adsorption capacity. *Lc* is an eco-friendly and sustainable adsorbent. It acts as a non-conventional material to reduce azo dyes dissolved in water. It could be applied to coupled treatments to ensure pollutant concentrations are sufficiently reduced and that wastewater treatment performs efficiently.

References

1. Holkar, C.R.; Jadhav, A.J.; Pinjari, D.V.; Mahamuni, N.M.; Pandit, A.B. A critical review on textile wastewater treatments: Possible approaches. *J. Environ. Manag.* **2016**, *182*, 351–366. [CrossRef] [PubMed]
2. Jan, S.U.; Ahmad, A.; Khan, A.A.; Melhi, S.; Ahmad, I.; Sun, G.; Ahmad, R. Removal of azo dye from aqueous solution by a low-cost activated carbon prepared from coal: Adsorption kinetics, isotherms study, and DFT simulation. *Environ. Sci. Pollut. Res.* **2021**, *28*, 10234–10247. [CrossRef] [PubMed]
3. Kakavandi, B.; Ahmadi, M. Efficient treatment of saline recalcitrant petrochemical wastewater using heterogeneous UV-assisted sono-Fenton process. *Ultrason. Sonochem.* **2019**, *56*, 25–36. [CrossRef] [PubMed]
4. Alwadani, N.; Fatehi, P. Synthetic and lignin-based surfactants: Challenges and opportunities. *Carbon Resour. Convers.* **2008**, *1*, 126–138. [CrossRef]
5. Di Maria, F.S.; Daskal, S.O.; Ayalon, O. A methodological approach for comparing wastewater effluent's regulatory and management frameworks based on sustainability assessment. *Ecol. Indic.* **2020**, *118*, 106805. [CrossRef]
6. Kubra, K.T.; Salman, M.S.; Hasan, M.N. Enhanced toxic dye removal from wastewater using biodegradable polymeric natural adsorbent. *J. Mol. Liq.* **2021**, *328*, 115468. [CrossRef]
7. Zhou, Y.; Lu, J.; Zhou, Y.; Liu, Y. Recent advances for dyes removal using novel adsorbents: A review. *Environ. Pollut.* **2019**, *253*, 352–365. [CrossRef] [PubMed]
8. Tantak, N.P.; Chaudhari, S. Degradation of azo dyes by sequential Fenton's oxidation and aerobic biological treatment. *J. Hazard. Mater.* **2006**, *136*, 698–705. [CrossRef] [PubMed]
9. Zaruma, P.; Proal, J.; Hernández, I.C.; Salas, H.I. Los colorantes textiles industriales y tratamientos óptimos de sus efluentes de agua residual: Una breve revisión. *Rev. La Fac. Cienc. Químicas* **2018**, *19*, 38–47.
10. Cabrera Rodríguez, E.; León Fernández, V.; Montano Pérez, A.C.; Dopico Ramírez, D. Caracterización de residuos agroindustriales con vistas a su aprovechamiento. *Cent. Azúcar* **2016**, *43*, 27–35.
11. Crini, G. Non-conventional low-cost adsorbents for dye removal: A review. *Bioresour. Technol.* **2006**, *97*, 1061–1085. [CrossRef] [PubMed]
12. Soares, A. Wastewater treatment in 2050, Challenges ahead and future vision in a European context. *Environ. Sci. Ecotechnol.* **2020**, *2*, 100030. [CrossRef] [PubMed]
13. Yaashikaa, P.R.; Kumar, P.S.; Saravanan, A.N.; Vo, D.V. Advances in biosorbents for removal of environmental pollutants: A review on pretreatment, removal mechanism and future outlook. *J. Hazard. Mater.* **2021**, *420*, 126596. [CrossRef] [PubMed]
14. Adewuyi, A.; Pereira, F.V. Underutilized *Luffa cylindrica* sponge: A local bio-adsorbent for the removal of Pb(II) pollutant from water system. *Beni-Suef Univ. J. Basic Appl. Sci.* **2017**, *6*, 118–126. [CrossRef]
15. Anastopoulos, I.; Pashalidis, I. Environmental applications of *Luffa cylindrica*-based. *J. Mol. Liq.* **2020**, *319*, 114127. [CrossRef]

16. Thomas, A. Functional materials: From hard to soft porous frameworks. *Angew. Chem. Int. Ed.* **2010**, *49*, 8328–8344. [CrossRef]

17. Soler-Illia, G.J.; Azzaroni, O. Multifunctional hybrids by combining ordered mesoporous materials and macromolecular building blocks. *Chem. Soc. Rev.* **2011**, *40*, 1107–1150. [CrossRef] [PubMed]

18. Slater, A.G.; Cooper, A.I. Function-led design of new porous materials. *Science* **2015**, *348*, 988. [CrossRef] [PubMed]

19. De la Cruz, P.; Melgoza, R.; Valerio, C.; Valladares, M. Adsorbentes noconvencionales, alternativas sustentables para el tratamiento de aguas residuales. *Rev. Ing. Univ. Medellín* **2017**, *16*, 55–73. [CrossRef]

20. Mohan Kumar, K.; Naik, V.; Kaup, V.; Waddar, S.; Santhosh, N.; Harish, H.V. Nontraditional Natural Filler-Based Biocomposites for Sustainable Structures. *Adv. Polym. Technol.* **2023**, *2023*, 8838766. [CrossRef]

21. El Naeem, G.A.; Abd-Elhamid, A.I.; Farahat, O.O.; El-Bardan, A.A.; Soliman, H.M.; Nayl, A.A. Adsorption of crystal violet and methylene blue dyes using a cellulose-based adsorbent from sugarcane bagasse: Characterization, kinetic and isotherm studies. *J. Mater. Res. Technol.* **2022**, *19*, 3241–3254. [CrossRef]

22. Jain, S.N.; Tamboli, S.R.; Sutar, D.S.; Jadhav, S.R.; Marathe, J.V.; Shaikh, A.A.; Prajapati, A.A. Batch and continuous studies for adsorption of anionic dye onto waste tea residue: Kinetic, equilibrium, breakthrough and reusability studies. *J. Clean. Prod.* **2020**, *252*, 119778. [CrossRef]

23. Lemos, E.S.; Fiorentini, E.F.; Bonilla-Petriciolet, A.; Escudero, L.B. Malachite green removal by grape stalks biosorption from natural waters and effluents. *Adsorpt. Sci. Technol.* **2023**, *2023*, 6695937. [CrossRef]

24. Rajoriya, S.; Saharan, V.K.; Pundir, A.S.; Nigam, M.; Roy, K. Adsorption of methyl red dye from aqueous solution onto eggshell waste material: Kinetics, isotherms and thermodynamic studies. *Curr. Res. Green Sustain. Chem.* **2021**, *4*, 100180. [CrossRef]

25. Kaya, A. Adsorption studies of Cibacron Blue onto both untreated and chemically treated pistachio shell powder from aqueous solutions. *Sep. Sci. Technol.* **2021**, *56*, 2546–2561. [CrossRef]

26. Abbas, M.; Harrache, Z.; Trari, M. Mass-transfer processes in the adsorption of crystal violet by activated carbon derived from pomegranate peels: Kinetics and thermodynamic studies. *J. Eng. Fibers Fabr.* **2020**, *15*, 1558925020919847. [CrossRef]

27. Brice, D.N.C.; Manga, N.H.; Arnold, B.S.; Daouda, K.; Victoire, A.A.; Giresse, N.N.A.; Nangah, C.R.; Nsami, N.J. Adsorption of tartrazine onto activated carbon based cola nuts shells: Equilibrium, kinetics, and thermodynamics studies. *Open J. Inorg. Chem.* **2021**, *11*, 1–9. [CrossRef]

28. Kesraoui, A.; Moussa, A.; Ali, G.B.; Seffen, M. Biosorption of alpacide blue from aqueous solution by lignocellulosic biomass: *Luffa cylindrica* fibers. *Environ. Sci. Pollut. Res.* **2016**, *23*, 15832–15840. [CrossRef] [PubMed]

29. Nadaroglu, H.; Cicek, S.; Gungor, A.A. Removing Trypan blue dye using nano-Zn modified *Luffa sponge*. *Spectrochim. Acta Part A Mol. Biomol. Spectrosc.* **2017**, *172*, 2–8. [CrossRef]

30. Boudechiche, N.; Mokaddem, H.; Sadaoui, Z.; Trari, M. Biosorption of cationic dye from aqueous solutions onto lignocellulosic biomass (*Luffa cylindrica*): Characterization, equilibrium, kinetic and thermodynamic studies. *Int. J. Ind. Chem.* **2016**, *7*, 167–180. [CrossRef]

31. Mashkoor, F.; Nasar, A. Preparation, characterization and adsorption studies of the chemically modified *Luffa aegyptica* peel as a potential adsorbent for the removal of malachite green from aqueous solution. *J. Mol. Liq.* **2019**, *274*, 315–327. [CrossRef]

32. Ng, H.W.; Lee, L.Y.; Chan, W.L.; Gan, S.; Chemmangattuvalappil, N. *Luffa acutangula* peel as an effective natural biosorbent for malachite green removal in aqueous media: Equilibrium, kinetic and thermodynamic investigations. *Desalination Water Treat.* **2016**, *16*, 7302–7311. [CrossRef]

33. Altınışık, A.; Gür, E.; Seki, Y. A natural sorbent, *Luffa cylindrica* for the removal of a model basic dye. *J. Hazard. Mater.* **2010**, *179*, 1–3. [CrossRef]

34. Manna, S.; Roy, D.; Saha, P.; Gopakumar, D.; Thomas, S. Rapid methylene blue adsorption using modified lignocellulosic materials. *Process. Saf. Environ. Prot.* **2017**, *107*, 346–356. [CrossRef]

35. Ajuru, M.; Nmom, F. A review on the economic uses of species of Cucurbitaceae and their sustainability in Nigeria. *Am. J. Plant. Biol.* **2017**, *2*, 17–24.

36. Emenea, A.; Akpanb, U.G.; Edyveana, R. Light-assisted adsorption of methylene blue dye onto *Luffa cylindrica*. *Desalination Water Treat.* **2021**, *216*, 379–388. [CrossRef]

37. Javadian, H.; Sorkhrodi, F.; Koutenaei, B. Experimental investigation on enhancing aqueous cadmium removal via nanostructure composite of modified hexagonal type mesoporous silica with polyaniline/polypyrrole nanoparticles. *J. Ind. Eng. Chem.* **2014**, *20*, 3678–3688. [CrossRef]

38. Crini, G.; Peindy, H.; Gimbert, F.; Robert, C. Removal of C.I. Basic Green 4 (malachite green) from aqueous solutions by adsorption using cyclodextrin based adsorbent: Kinetic and equilibrium studies. *Sep. Purif. Technol.* **2007**, *53*, 97–110. [CrossRef]

39. Saeed, A.; Iqbal, M.; Zafar, I. Immobilization of Trichoderma viride for enhanced methylene blue biosorption: Batch and column studies. *J. Hazard. Mater.* **2009**, *168*, 406–415. [CrossRef]

40. Han, R.; Wang, Y.; Han, P.; Shi, J.; Yang, J.; Lu, Y. Removal of methylene blue from aqueous solution by chaff in batch mode. *J. Hazard. Mater.* **2006**, *B137*, 550–557. [CrossRef]

41. Sims, R.A.; Harmer, S.L.; Quinton, J.S. The role of physisorption and chemisorption in the oscillatory adsorption of organosilanes on aluminium oxide. *Polymers* **2019**, *11*, 410. [CrossRef] [PubMed]

42. Shakoor, S.; Nasar, A. Removal of methylene blue dye from artificially contaminated water using *Citrus limetta* peel waste as a very low-cost adsorbent. *J. Taiwan Inst. Chem. Eng.* **2016**, *66*, 154–163. [CrossRef]

43. Aliabadi, H.; Saberikhah, E.; Pirbazari, A.; Khakpour, R.; Alipour, H. Triethoxysilylpropylamine modified alkali treated wheat straw: An efficient adsorbent for methyl orange adsorption. *Cellul. Chem. Technol.* **2018**, *52*, 129–140.
44. Liang, J.; Wu, J.; Li, P.; Wang, X.; Yang, B. Shaddock peel as a novel low-cost adsorbent for removal of methylene blue from dye wastewater. *Desalination Water Treat.* **2012**, *39*, 70–75. [CrossRef]
45. Gong, W.Q.; Zhou, Q.; Xie, C.X.; Yuan, X.A.; Li, Y.B.; Bai, C.P.; Chen, S.H.; Xu, N.A. Biosorption of Methylene Blue from aqueous solution on spent cottonseed hull substrate for *Pleurotus ostreatus* cultivation. *Desalination Water Treat.* **2011**, *29*, 317–325. [CrossRef]
46. Sharma, R.K.; Kumar, R. Functionalized cellulose with hydroxyethyl methacrylate and glycidyl methacrylate for metal ions and dye adsorption applications. *Int. J. Biol. Macromol.* **2019**, *134*, 704–721. [CrossRef] [PubMed]
47. Al-Ghouti, M.A.; Da'ana, D.A. Guidelines for the use and interpretation of adsorption isotherm models: A review. *J. Hazard. Mater.* **2020**, *392*, 122382. [CrossRef]
48. Anastopoulos, I.; Pashalidis, I. The application of oxidized carbon derived from Luffa cylindrica for caffeine removal. Equilibrium, thermodynamic, kinetic and mechanistic analysis. *J. Mol. Liq.* **2019**, *296*, 112078. [CrossRef]
49. Mckay, G.B.H.S.; Blair, H.S.; Gardner, J.R. Adsorption of dyes on chitin. I. Equilibrium studies. *J. Appl. Polym. Sci.* **1982**, *27*, 3043–3057. [CrossRef]
50. Oliveira, E.A.; Montanher, S.F.; Rollemberg, M.C. Removal of textile dyes by sorption on low-cost sorbents. A case study: Sorption of reactive dyes onto *Luffa cylindrica*. *Desalination Water Treat.* **2011**, *25*, 54–64. [CrossRef]
51. Zulkefli, S.; Abdulmalek, E.; Rahman, M.B.A. Pretreatment of oil palm trunk in deep eutectic solvent and optimization of enzymatic hydrolysis of pretreated oil palm trunk. *Renew. Energy* **2017**, *107*, 36–41. [CrossRef]
52. Rosli, M.I.; Abdullah, M.; Krishnan, G.; Harun, S.W.; Aziz, M.S. Power-dependent nonlinear optical behaviours of ponceau BS chromophore at 532 nm via Z-scan technique. *J. Photochem. Photobiol. A Chem.* **2020**, *397*, 112574. [CrossRef]
53. Bellamy, L.J. *The Infrared Spectra of Complex Molecules*, 3rd ed.; Springer Science & Business Media: London, UK, 2013; Volume II, pp. 303–315.
54. Al-Ghouti, M.; Hawari, A.; Khraisheh, M. A solid-phase extractant based on microemulsion modified date pits for toxic pollutants. *J. Environ. Manag.* **2013**, *130*, 80–89. [CrossRef] [PubMed]
55. El-Hendawy, A.N.A. Variation in the FTIR spectra of a biomass under impregnation, carbonization and oxidation conditions. *J. Anal. Appl. Pyrolysis* **2006**, *72*, 159–166. [CrossRef]
56. Ighalo, J.O.; Adeniyi, A.G.; Oke, E.O.; Adewoye, L.T.; Motolani, F.O. Evaluation of *Luffa cylindrica* fibers in a bio-mass packed bed for the treatment of paint industry effluent before environmental release. *Eur. J. Sustain. Dev. Res.* **2020**, *4*, em0132. [CrossRef] [PubMed]
57. Collins, M.N.; Nechifor, M.; Tanasă, F.; Zănoagă, M.; McLoughlin, A.; Stróżyk, M.A.; Culebras, M.; Teacă, C.A. Valorization of lignin in polymer and composite systems for advanced engineering applications: A review. *Int. J. Biol. Macromol.* **2019**, *131*, 828. [CrossRef] [PubMed]
58. Wakkel, M.; Khiari, B.; Zagrouba, F. Textile wastewater treatment by agro-industrial waste: Equilibrium modelling, thermodynamics and mass transfer mechanisms of cationic dyes adsorption onto low-cost lignocellulosic adsorbent. *J. Taiwan Inst. Chem. Eng.* **2019**, *96*, 439–452. [CrossRef]
59. Crini, G. Recent developments in polysaccharide-based materials used as adsorbents in wastewater treatment. *Prog. Polym. Sci.* **2005**, *30*, 30–70. [CrossRef]
60. Cardoso, N.; Lima, E.; Pinto, I.; Amavisca, C.; Royer, B.; Pinto, R.; Alencar, W.; Pereira, S. Application of Cupuassu shell as biosorbent for the removal of textile dyes from aqueous solution. *J. Environ. Manag.* **2011**, *92*, 1237–1247. [CrossRef]
61. Alencar, W.; Lima, E.; Royer, B.; Dos Santos, B.; Calvete, T.; Da Silva, E.; Alves, C. Application of aqai stalks as biosorbents for the removal of the dye Procion Blue MX-R from aqueous solution. *Sep. Sci. Technol.* **2012**, *47*, 513–526. [CrossRef]
62. Cardoso, N.; Lima, E.; Calvete, T.; Pinto, I.; Amavisca, C.; Fernandes, T.; Pinto, R.; Alencar, W. Application of aqai stalks as biosorbents for the removal of the dyes Reactive Black 5 and Reactive Orange 16 from aqueous solution. *J. Chem. Eng. Data* **2011**, *56*, 1857–1858. [CrossRef]
63. Khadir, A.; Motamedi, M.; Pakzad, E.; Sillanpää, M.; Mahajan, S. The prospective utilization of *Luffa* fibres as a lignocellulosic bio-material for environmental remediation of aqueous media: A Review. *J. Environ. Chem. Eng.* **2021**, *9*, 104691. [CrossRef]
64. Karaghool, H.A.; Hashim, K.; Kot, P.; Muradov, M. Preliminary Studies of Methylene Blue Remotion from Aqueous Solutions by *Ocimum basilicum*. *Environments* **2022**, *9*, 17. [CrossRef]
65. Mall, I.; Srivastava, V.; Kumar, G.; Mishra, I. Characterization and utilization of mesoporous fertilizer plant waste carbon for adsorptive removal of dyes from aqueous solution. *Colloids Surf.* **2006**, *278*, 175–187. [CrossRef]
66. El Kassimi, A.; Achour, Y.; El Himri, M.; Laamari, R.; El Haddad, M. Removal of two cationic dyes from aqueous solutions by adsorption onto local clay: Experimental and theoretical study using DFT method. *Int. J. Environ. Anal. Chem.* **2023**, *103*, 1223–1224. [CrossRef]
67. Jaafari, J.; Barzanouni, H.; Mazloomi, S.; Farahani, N.A.A.; Sharafi, K.; Soleimani, P.; Haghighat, G.A. Effective adsorptive removal of reactive dyes by magnetic chitosan nanoparticles: Kinetic, isothermal studies and response surface methodology. *Int. J. Biol. Macromol.* **2020**, *164*, 344–355. [CrossRef] [PubMed]
68. Debord, J.; Harel, M.; Bollinger, J.C.; Chu, K.H. The Elovich isotherm equation: Back to the roots and new developments. *Chem. Eng. Sci.* **2022**, *262*, 118012. [CrossRef]

69.   Langmuir, I. The adsorption of gases on plane surfaces of glass, mica and platinum. *J. Am. Chem. Soc.* **1918**, *40*, 1361–1403. [CrossRef]

70.   Said, K.A.M.; Ismail, N.Z.; Jama'in, R.L.; Alipah, N.A.M.; Sutan, N.M.; Gadung, G.G.; Baini, R.; Zauzi, N.S.A. Application of Freundlich and Temkin isotherm to study the removal of Pb(II) via adsorption on activated carbon equipped polysulfone membrane. *Int. J. Eng. Technol.* **2018**, *7*, 91–93. [CrossRef]